Observation of Polymer Conformation Hysteresis in Extensional Flow

Charles M. Schroeder *et al.*

Science **301**, 1515 (2003);
DOI: 10.1126/science.1086070

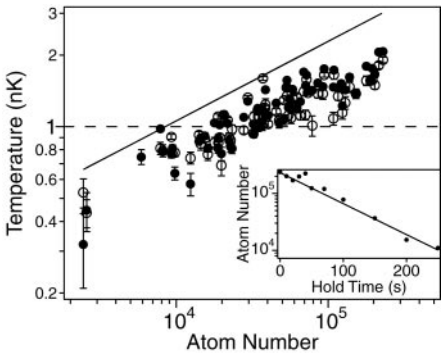

Fig. 3. Bose-Einstein condensates at picokelvin temperatures. The temperature of more than 60 partially condensed atomic vapors is plotted versus total number of condensed and noncondensed atoms. A solid line at the Bose-Einstein condensation phase transition temperature (Eq. 1) and a dashed line at 1 nK are provided as guides. Condensate temperatures were determined from one-dimensional fits to atomic density cross sections integrated along either the *x* (closed circles) or *y* (open circles) axis (Fig. 2). Differences in the two measured temperatures for a single condensate reflect the true uncertainty of the measurement. Plotted error bars represent the statistical uncertainty of the fit. The inset shows that the 1/*e* condensate lifetime in the gravito-magnetic trap was limited by one-body processes to 80 ± 5 s.

$w_{th} = (2k_B T / m\omega^2)^{1/2}$, in any spatial direction can be related to the temperature, provided that the thermal energy is much larger than the trap level spacing, $k_B T \gg \hbar \bar{\omega}$, where ω is the trap frequency for the axis along which w_{th} is measured (*22*). The ratio of atoms in the condensate, N_0, to the total number of atoms, $N = N_0 + N_{th}$, is also related to the temperature through $N_0/N = 1 - (T/T_c)^3$. N_0, N_{th}, and w_{th} are therefore completely determined by T and N.

The temperature of the atomic vapors was extracted by fitting integrated, one-dimensional atomic density cross sections to a bimodal distribution (Fig. 2)

$$n(x) = N_0\Psi_0^2 + \frac{N_{th}}{\sqrt{\pi} w_{th}} e^{-x^2/w_{th}^2} \quad (2)$$

where Ψ_0^2 is a bell-shaped function with width w_0 that describes the condensate peak [$\Psi_0^2 = (15/16)\, w_0^{-1} \max(1 - x^2/w_0^2, 0)^2$ for a Thomas-Fermi gas and $\Psi_0^2 = w_0^{-1}\pi^{-1/2} \exp(-x^2/w_0^2)$ for an ideal gas]. The fitted parameters were T, N, and w_0. We checked that the fitted temperature did not depend on the exact choice of the condensate wave function (inverted parabola or gaussian) or the application of microwave radiation to reduce atom number.

All atomic vapors represented in Fig. 3 had a clear bimodal density distribution from which a temperature was reproducibly extracted. The temperatures extracted from one-dimensional fits along both radial axes were nominally the same, empirically indicating that the atomic vapors remained close to thermal equilibrium at all times.

In conclusion, we have created long-lived (80 ± 5 s), low-temperature (450 ± 80 pK), and low-density (5×10^{10} atoms/cm^3) partially condensed atomic vapors using a weakly confining [$\varpi = 2\pi \times (1.12 \pm 0.08)$ Hz] gravito-magnetic trap. These samples are characterized by a thermal velocity ~1 mm/s, a speed of sound ~100 μm/s, and a healing length limited by the ~20-μm harmonic oscillator length of the trapping potential. Low-temperature and low-density ensembles are important for spectroscopy, metrology, and atom optics. In addition, they are predicted to experience quantum reflection from material surfaces (*26–28*).

References and Notes

1. H. G. Smith, J. O. Wilhelm, *Rev. Mod. Phys.* **7**, 237 (1935).
2. K. Darrow, *Rev. Mod. Phys.* **12**, 257 (1940).
3. S. Chu, *Rev. Mod. Phys.* **70**, 685 (1998).
4. C. N. Cohen-Tannoudji, *Rev. Mod. Phys.* **70**, 707 (1998).
5. W. D. Phillips, *Rev. Mod. Phys.* **70**, 721 (1998).
6. E. A. Cornell, C. E. Wieman, *Rev. Mod. Phys.* **74**, 875 (2002).
7. W. Ketterle, *Rev. Mod. Phys.* **74**, 1131 (2002).
8. B. DeMarco, D. S. Jin, *Science* **285**, 1703 (1999).
9. A. H. Silver, J. E. Zimmerman, *Phys. Rev. Lett.* **15**, 888 (1965).
10. K. Schwab, N. Bruckner, R. E. Packard, *Nature* **386**, 585 (1997).
11. O. Avenel, P. Hakonen, E. Varoquaux, *Phys. Rev. Lett.* **78**, 3602 (1997).
12. T. Udem, R. Holzwarth, T. W. Hänsch, *Nature* **416**, 233 (2002).
13. A. S. Oja, O. V. Lounasmaa, *Rev. Mod. Phys.* **69**, 1 (1997).
14. M. Kasevich, S. Chu, *Phys. Rev. Lett.* **69**, 1741 (1992).
15. J. Reichel *et al.*, *Phys. Rev. Lett.* **75**, 4575 (1995).
16. B. Saubaméa *et al.*, *Phys. Rev. Lett.* **79**, 3146 (1997).
17. M.-O. Mewes *et al.*, *Phys. Rev. Lett.* **77**, 416 (1996).
18. T. Weber, J. Herbig, M. Mark, H.-C. Nägerl, R. Grimm, *Science* **299**, 232 (2003).
19. A. Kastberg, W. D. Phillips, S. L. Rolston, R. J. C. Spreeuw, *Phys. Rev. Lett.* **74**, 1542 (1995).
20. P. Treutlein, K. Y. Chung, S. Chu, *Phys. Rev. A* **63**, 051401(R) (2001).
21. E. A. Donley, N. R. Claussen, S. T. Thompson, C. E. Wieman, *Nature* **417**, 529 (2002).
22. F. Dalfovo, S. Giorgini, L. P. Pitaeskii, S. Stringari, *Rev. Mod. Phys.* **71**, 463 (1999).
23. T. L. Gustavson *et al.*, *Phys. Rev. Lett.* **88**, 020401 (2002).
24. Y. V. Gott, M. S. Ioffe, V. G. Tel'kovskii, *Nuc. Fus. Suppl.* **3**, 1045 (1962).
25. D. E. Pritchard, *Phys. Rev. Lett.* **51**, 1336 (1983).
26. A. Anderson *et al.*, *Phys. Rev. A* **34**, 3513 (1986).
27. J. J. Berkhout *et al.*, *Phys. Rev. Lett.* **63**, 1689 (1989).
28. F. Shimizu, *Phys. Rev. Lett.* **86**, 987 (2001).

29. This work was funded by the Army Research Office, NSF, Office of Naval Research, and NASA. We thank C. V. Nielsen for experimental assistance and J. K. Thompson for critical comments on the manuscript. M.S. acknowledges additional support from the Swiss National Science Foundation.

7 July 2003; accepted 12 August 2003

Observation of Polymer Conformation Hysteresis in Extensional Flow

Charles M. Schroeder,[1] Hazen P. Babcock,[2]* Eric S. G. Shaqfeh,[1,3] Steven Chu[2]†

Highly extensible *Escherichia coli* DNA molecules in planar extensional flow were visualized in dilute solution by fluorescence microscopy. For a narrow range of flow strengths, the molecules were found in either a coiled or highly extended conformation, depending on the deformation history of the polymer. This conformation hysteresis persists for many polymer relaxation times and is due to conformation-dependent hydrodynamic forces. Polymer conformational free-energy landscapes were calculated from computer simulations and show two free-energy minima for flow strengths near the coil-stretch transition. Hysteresis cycles may directly influence bulk-solution stresses and the development of stress-strain relations for dilute polymer flows.

The behavior of long-chain, flexible polymer molecules in extension-dominated flows has been the subject of research discussion for more than 30 years (*1*). Flows of dilute polymer solutions exhibit several interesting macroscopic effects including flow-dependent viscosity, enhanced normal stresses, and turbulent-drag reduction. Such non-Newtonian fluid properties result from flow-induced changes in the polymer conformations in solution. In short, a flowing fluid will influence polymer configurations in solution, and the forces exerted back on the fluid are directly related to the molecular conformations.

Polymer conformations and the resultant bulk-solution stresses are affected by flow type. In general, flows with a large rotational

[1]Department of Chemical Engineering, [2]Departments of Physics and Applied Physics, [3]Department of Mechanical Engineering, Stanford University, Stanford, CA 94305, USA.

*Present address: Department of Chemistry and Chemical Biology, Harvard University, Cambridge, MA 02138, USA.

†To whom correspondence should be addressed. E-mail: schu@stanford.edu

component tend not to perturb polymer configurations far from the equilibrium coiled state. However, flows with a dominant extensional component may substantially orient and stretch polymers (*2*). From a practical standpoint, extensional flows are realized in many polymer-processing applications, including coating, injection molding, and fiber drawing.

A planar (two-dimensional) extensional flow is described by a line of pure fluid extension and an orthogonal line of pure fluid compression. Components of the fluid velocity (v_x, v_y) in the directions of the extensional and compressional axes vary linearly with position such that $v_x = \dot{\varepsilon}x$ and $v_y = -\dot{\varepsilon}y$, where $\dot{\varepsilon}$ is the strain rate. Planar extensional flow exhibits no rotational components and therefore has the ability to drastically stretch flexible polymer chains even at low flow strengths.

An abrupt coil-stretch transition for polymers in extensional flows is predicted to occur at dimensionless flow strengths $De \approx 0.5$ (*3*), where the Deborah number, $De \equiv \tau_r\dot{\varepsilon}$, is the ratio of two intrinsic time scales: the longest polymer relaxation time (τ_r) and the characteristic fluid stretching time ($\dot{\varepsilon}^{-1}$). The width of the coil-stretch transition is expected to scale inversely with the contour length of the polymer, so in the limit of very long polymers, the transition is very sharp (*4*). Experiments based on optical techniques, including birefringence (*5*, *6*) and light scattering (*7*, *8*), have previously been used to infer polymer stretch and orientation. These traditional experiments revealed useful information regarding polymer conformations in solution, but the average behavior of a large ensemble of polydisperse molecules revealed a broad transition from a coiled to extended state. With the advent of single-molecule observations, even monodisperse samples revealed a large variance in the time it took the molecules to reach their equilibrium extension (*9*, *10*). When the extension of only those molecules that reached their equilibrium length is plotted as a function of *De*, the transition from coiled to stretched state occurred near $De = 0.5$ and became more than an order of magnitude sharper than previous observations.

In 1974, de Gennes predicted the existence of a hysteresis cycle in steady-state polymer extension near the critical transition in extensional flows (*4*). He argued that the hydrodynamic force exerted by the fluid on the polymer would increase as a polymer molecule stretched from its equilibrium coiled state. In the coiled state, interior monomer units are hydrodynamically shielded from the full velocity field as a result of nearby portions of the same polymer chain. However, as the molecule stretches, the fluid is able to exert a stronger frictional grip. Using simple polymer kinetic theory, de Gennes arrived at an S-shaped curve for the steady-state polymer extension versus *De* (Fig. 1) and argued that in a narrow range of flow strengths near the coil-stretch transition, three molecular configurations were possible: a highly stretched "S" state, a compacted coiled "C" state, and a physically unstable "P" configuration.

The behavior of long-chain polymers near this phase transition has been a highly debated topic for several decades. Although the notion of conformation hysteresis was supported by Hinch and Tanner around the same time as de Gennes' proposal (*11*–*16*), in 1985, Fan *et al*. (*17*) argued that de Gennes' S-shaped extension curve was nonphysical and could only arise as the result of mathematical approximations. Wiest *et al*. (*18*) broadened the argument against hysteresis with computer simulations of polymers and found no evidence of hysteresis, concluding that de Gennes' S-shaped curves were indeed nonphysical.

The existence of polymer conformation hysteresis in the coil-stretch transition has important implications with regard to our understanding of phase transitions. The static and dynamic properties of polymers have striking similarities with critical phenomena in many-body systems (*19*). In the limit of long polymers, the topological transition between extended and coiled states of a polymer is related to a phase transition between different states of matter where the effective temperature of the system scales as $1/M$, where M is the molecular weight of the polymer. For example, consider the classic liquid-vapor phase transition (*20*). Figure 2A shows the pressure–molar volume relation for a substance with the three curves corresponding to different temperatures such that $T_1 < T_2 < T_3$. Below a critical temperature $\sim T_2$, a cubic equation of state (such as van der Waals) gives isotherms (such as T_1) where liquid and vapor phases can coexist as an inhomogeneous mixture of two states with well-defined molar volumes. Saturated vapors can be subcooled into metastable states in the absence of liquid nucleation sites; similarly, saturated liquids may be superheated into the two-phase region specified by the dotted line. In both cases, the system is kinetically trapped in a local minimum of free energy. The presence of hysteresis is a signature of a first-order phase transition with an associated latent heat.

By analogy, polymers above a critical length M_2 can exist in two stable states of

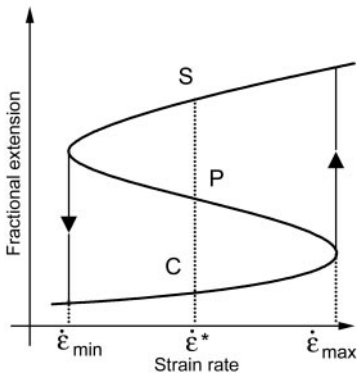

Fig. 1. Sketch of de Gennes' classic steady-state extension curve for polymers in extensional flow. De Gennes argued that polymers could exist in two physically realizable states (a stretched "S" and coiled "C" state) in a narrow range of flow strengths. The coiled and stretched polymer configurations correspond to free-energy minima E/kT in a double-welled potential, separated by an energy barrier with a maximum at extension "P." If a coiled polymer is exposed to an adiabatic increase in the strain rate, there would exist a particular $\dot{\varepsilon} = \dot{\varepsilon}^*$ at which $E^C/kT = E^S/kT$, at which the polymer would spend equal amounts of time in the coiled and stretched states. However, given the limited residence and observation times for polymers in extensional flows, a hysteresis in extension would occur for most practical situations for $\dot{\varepsilon}$ between $\dot{\varepsilon}_{min}$ and $\dot{\varepsilon}_{max}$.

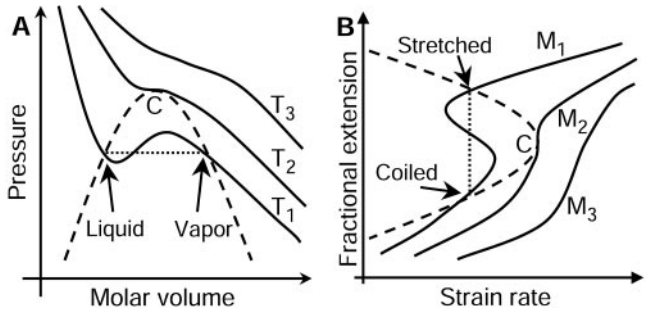

Fig. 2. (**A**) Classic first-order phase transition for vaporization or fusion of a pure substance. For temperatures T less than a critical temperature T_2, vapor and liquid phases may coexist along an isotherm T_1 where the molar free energies of the liquid and vapor phases are equal. A cubic equation of state is merely an approximation to actual phase behavior (dashed line). (**B**) Coil-stretch phase transition for flexible polymers in extensional flows. For linear polymers with molecular weights M_1 greater than a critical molecular weight M_2, configuration hysteresis is possible in a range of *De*. Clearly, the steady-state extension will be a function of the deformation history of the polymer. The coil-stretch transition (given by the vertical dotted line) may be defined at the strain rate where the configurational free energies of the stretched and coiled states are equal for $M > M_2$.

extension corresponding to coiled and extended configurations (Fig. 2B). Because we are considering a single molecule, the simultaneous coexistence of two different conformations is not meaningful. However, a polymer in an initially extended (coiled) state can remain kinetically trapped in the extended (coiled) configuration. If hysteresis is found to exist, the coil-stretch transition must be a first-order transition.

If the hydrodynamic drag forces on a stretched polymer were orders of magnitude greater than the drag on a coil, one could argue on intuitive grounds that hysteresis would be likely. The hydrodynamic drag resistivity (ζ^{coil}) for a coiled polymer is expected to scale as the radius of gyration R_g, so that $\zeta^{coil} \sim N^{\nu}$, where N is the number of statistical Kuhn segments and $\nu = 0.5$ or 0.6, depending on solvent conditions. In contrast, the drag resistivity of a long, slender body (*21*) in viscous flow ($\zeta^{stretch}$) is

$$\zeta^{stretch} \approx N/\ln(L/b) \quad (1)$$

where b is the hydrodynamic radius of a monomer unit (*22*). In the limit of very long polymers, $\zeta^{stretch}/\zeta^{coil}$ weakly diverges and hysteresis becomes plausible. The crucial question is how much greater must $\zeta^{stretch}$ be compared with ζ^{coil} for hysteresis to occur. For λ-DNA (~150 Kuhn segments), R_g = 0.73 μm (*23*) and the fluorescently stained contour length is 21.1 μm (*24*), such that $\zeta^{stretch}/\zeta^{coil}$ is ~1.7. For DNA of ~2250 Kuhn segments, we estimate that $\zeta^{stretch}/\zeta^{coil}$ is only ~3.3. DNA is unusual when compared with synthetic polymers, because the ratio L/b is unusually large and the logarithm term in the denominator cannot be ignored.

We report here the direct observation of vastly separated coiled and stretched polymer configurations at identical flow strengths (*25*). We examined genomic-length DNA polymer chains with contour lengths L from 1.3 to 1.7 mm stained with a fluorescent dye (*26*). We were able to trap and image individual molecules in extensional flows for many hours with a flow cell (fig. S1), so that sizable strain ($\varepsilon = \dot{\varepsilon} t_{obs}$) can accumulate. The molecular trap is based on a flow cell where the position of the stagnation point is adjustable. If the molecule begins to drift toward one of the two exit ports, the flow impedance in the exit ports is adjusted so that the position of the stagnation point would reverse the direction of the drifting molecule (*26*). Our device is analogous to one used by Bentley and Leal to control the position of a fluid drop in a four-roll mill device (*27*). The long observation times of each DNA molecule required special measures (*26*) that provided long-term stability of the polymer physical properties, including contour length and relaxation time (*28*).

The hysteresis experiment was conducted by first trapping a polymer molecule and measuring its relaxation time with video microscopy. The molecule was then kept in zero-flow conditions for several relaxation times τ_r to ensure a random initial configuration. The polymer was then exposed to extensional flow at a particular *De* for several strain units. Next, we extended the same polymer at $De \geq 5$ and slowly decreased the pump speed to introduce the molecule to the same *De* value. After monitoring the extension for at least 10 units of Hencky strain (~30 relaxation times), we repeated the process for a flow with a slightly different *De* number. DNA molecules ~575 μm long were examined first (Fig. 3A). Conformation hysteresis was not observed at any *De* for this set of molecules. Trajectories for initially extended polymers with $L \approx 575$ μm were sluggish to recoil, and we conjecture that the effective energy potential may be flattening at this *De*, potentially signaling an approach to separated, bistable states.

Figure 3, B to D, shows the transient extension for DNA molecules with $L \approx$ 1300 μm when *De* is 0.30, 0.45, and 0.57. For low *De* values of ~0.30 (Fig. 3B), the hydrodynamic force exerted on the polymer is not sufficient to maintain an extended configuration. However, at $De = 0.45$, initially extended polymer molecules evolve to extensions of ≈ 670 μm and remain extended above 13 units of strain (Fig. 3C and fig. S3). The same molecule prepared in an initially coiled state remains at extensions near 41 μm over the course of 12 strain units, during which time fluid ele-

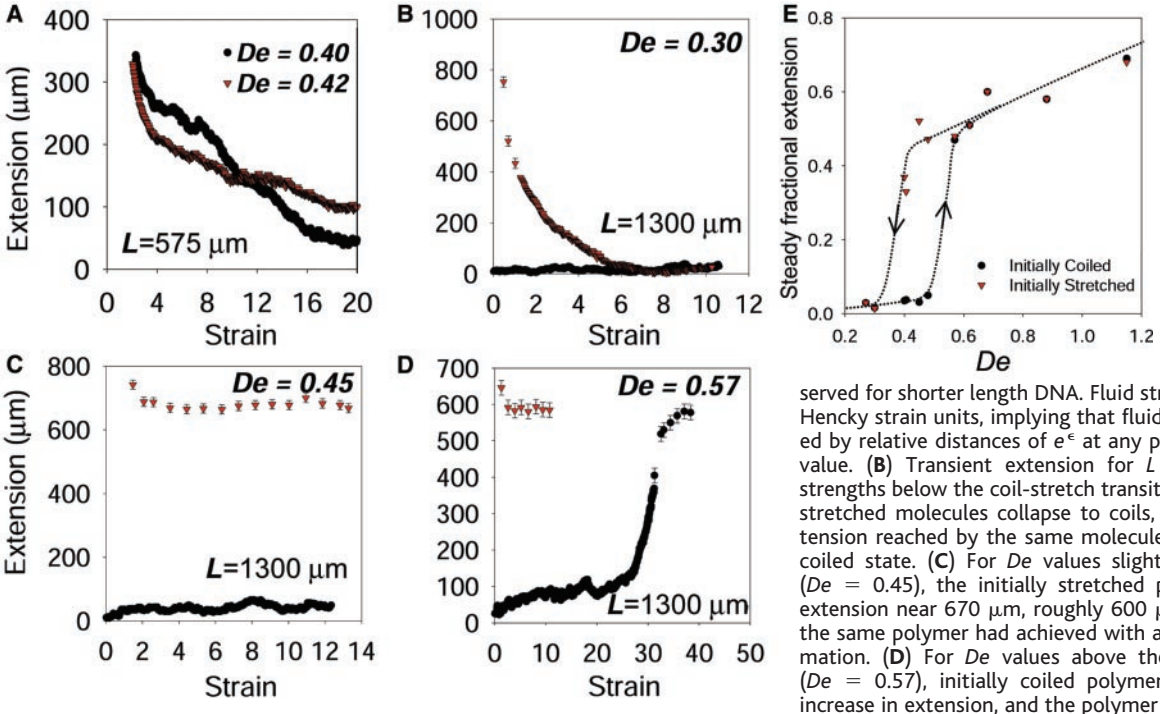

Fig. 3. Transient and steady molecular extension for DNA in planar extensional flow. (**A**) For $L \approx 575$ μm, no conformational hysteresis was observed at any *De*. Initially stretched molecules at $De \approx 0.4$ were slow to recoil with apparent local plateaus and shoulders in transient extension trajectories, generally not observed for shorter length DNA. Fluid strains (ε) are expressed in Hencky strain units, implying that fluid elements have separated by relative distances of e^{ϵ} at any particular transient strain value. (**B**) Transient extension for $L \approx 1300$ μm. At flow strengths below the coil-stretch transition ($De = 0.30$), initially stretched molecules collapse to coils, achieving the same extension reached by the same molecule prepared in an initially coiled state. (**C**) For *De* values slightly below the transition ($De = 0.45$), the initially stretched polymer reaches a final extension near 670 μm, roughly 600 μm more extended than the same polymer had achieved with an initially coiled conformation. (**D**) For *De* values above the coil-stretch transition ($De = 0.57$), initially coiled polymers experience a gradual increase in extension, and the polymer eventually unravels to a final length around 580 μm for fluid strains of 25. (**E**) Steady-state polymer extension as a function of $De = \varepsilon\tau_r$ for molecules with contour lengths of $L \approx 1.3$ mm (~9250 Kuhn segments). A distinct region of bistable polymer configuration is evident. The dashed line illustrates the hysteretic polymer cycle and is added to guide the eye. Individual observation times were long (≥1 hour), so the size of error bars are on the order of the symbol sizes. The corresponding steady extension plot for λ-DNA (L = 21 μm with ~150 Kuhn segments) (*9*) is single valued.

ments have separated by a relative distance of e^{12}, where e is the natural experimental function. These states remained distinct and were separated by an extension of ~630 μm, which is ~1/2 L for more than 30 relaxation times. At this De, our data indicate that two local energy minima exist for the polymer chain extension, and the energy barrier height is several kT, where kT is thermal energy, such that a random Brownian fluctuation does not cause either state to become unpopulated over the course of $\varepsilon = 12$ ($t_{obs} \approx 1$ hour).

Finally, we probed the transient dynamics of long-chain polymer molecules for De greater than the critical value. For $De = 0.57$ (Fig. 3D), the molecule initially prepared in the coiled state eventually unraveled to equivalent extensions for the initially extended polymer. Unlike trajectories for $De \leq 0.5$, the initially coiled state exhibited a nearly monotonic increase in extension up to ~100 μm at $\varepsilon = 10$. Slight perturbations in conformation were causing the monomer units to become unshielded to the flow, gradually enhancing the hydrodynamic drag exerted on the polymer by the solvent. Eventually, the molecule became sufficiently free draining and unraveled to a steady extension of ~580 μm.

We measured the extension of several polymer molecules with $L \approx 1.3$ mm at different De values near the critical region. The steady-state extension at different De values is shown in Fig. 3E, where each data point represents the time-averaged steady extension achieved by the polymer over the course of at least 8 to 10 strain units. The appearance of single values of extension for a given De number is a consequence of the initially coiled and stretched conformations achieving the same steady extension. A clear hysteresis region is revealed in which the polymer extension is a strong function of deformation history. Although the hysteresis region occurs over a narrow region of De values, the states are separated by several hundred micrometers of extension and persist for $\varepsilon \geq 10$, corresponding to hours of observation. Unexpectedly, only a modest change in the drag ratio is needed to produce hysteresis: We estimate that $\zeta^{stretch}/\zeta^{coil} \cong 5$ for 1.3-mm-long polymers. The effect of physical confinement of the DNA in the flow channel on the drag ratio is small (supporting online material text and fig. S2).

Computer simulations of polymer molecules modeled as a series of beads connected by springs were conducted with Brownian dynamics techniques (*29*, *30*). Hydrodynamic interaction effects were incorporated by using a point-force (Rotne-Prager-Yamakawa) interaction between beads along the polymer chain (*31*). In this model, the disturbance velocity experienced by one bead as a result of a neighboring bead decays to zero as the distance between them grows large. Simulations of polymer chains with $L \approx 1.3$ mm, corresponding to ≈9280 statistical Kuhn segments, were carried out in the same manner as the experiment. Single molecules were initialized in both a randomly coiled and a stretched state at equivalent values of De. Conformation hysteresis is apparent (Fig. 4A). The hysteresis is due solely to intramolecular hydrodynamic interactions, because we have not included effects due to physical boundaries confining the polymers.

Polymer chain resistivity, ζ^{chain}, as a function of polymer stretch (R), was also extracted from the simulations by coarse graining the internal modes of the multibead spring chain into a simple dumbbell. We calculated the conformational free energy as a function of extension for these large polymers using the $\zeta^{chain}(R)$ functionality. For small De below the coil-stretch transition, only one minimum in the free-energy landscape exists, corresponding to the coiled state. As De increases above values of 0.5, a single minimum exists at large extension, indicating the highly elongated polymer state. The conformational free energy is plotted in Fig. 4B for a narrow range of De near the coil-stretch transition. In this range of De, two shallow minima exist in the free energy landscape, giving rise to metastable polymer configurations at a single De, and hence conformation hysteresis. If the extrema in the polymer energy landscape are plotted as a function of De, an S-shape curve very similar to de Gennes' original plot of steady-state extension versus flow strength is recovered. The middle branch in the "S" represents the physically unstable configuration and "is the analog of the maximum point in a static potential barrier" (*4*).

We argue that the coiled and stretched polymer configurations in the hysteretic region are kinetically separated. The free-energy barrier separating the two states is typically much larger than kT, and random Brownian fluctuations were not strong enough to cause the polymer molecules to make transitions between coiled and extended states during the course of our observation. However, given a much longer observation time, the molecule may spend a fraction of time in both states, depending on the height of the barrier and the relative energy position of the coiled and stretched wells.

In addition to the implications of hysteresis with regard to first-order conformational phase transitions, hysteresis cycles may also have practical implications. For example, the extensional viscosity η^{ext} of a dilute polymer solution may be substantially larger (by a factor of 10^3 or 10^4) for a "prestretched" sample that had experienced a step strain in its processing history (*12*), imparting a larger viscous contribution to the total solution stress resulting from the long, extended portions of the polymer molecules. With hysteresis, the steady-state conformation of a polymer in flow becomes a function of its processing history, and steady-state solutions that neglect transient behavior become ambiguous (*12*). Our results suggest that hydrodynamic interac-

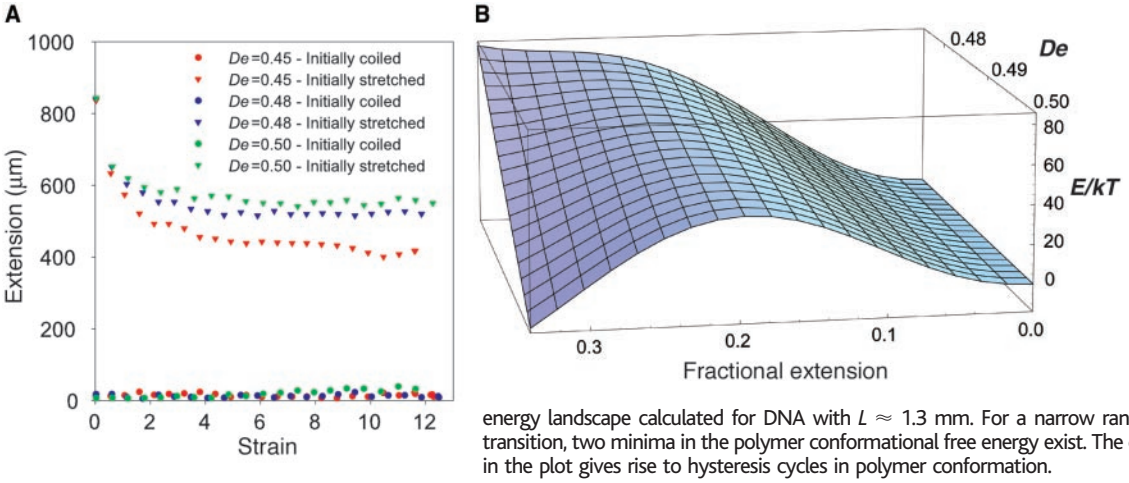

Fig. 4. Computer simulations of polymer molecules using Brownian dynamics techniques. **(A)** Transient molecular extention compared with Hencky strain for DNA consisting of ~9280 Kuhr segments with $L \approx 1.3$ mm. Initially stretched molecules (75% of the contour length) evolve to extensions several hundred micrometers greater than initially coiled polymers, as observed in the experiment. **(B)** Polymer conformational free energy landscape calculated for DNA with $L \approx 1.3$ mm. For a narrow range of De near the coil-stretch transition, two minima in the polymer conformational free energy exist. The double-walled potential shown in the plot gives rise to hysteresis cycles in polymer conformation.

tions should be an important feature of polymer theories attempting to model stresses in extensional flows. We anticipate that the effects of hydrodynamic interactions will be crucial for description of more flexible synthetic polymers such as polystyrene, with a smaller ratio of persistence length to hydrodynamic radius, and hence larger extensibility (L/R_g) ratios.

Finally, conformational hysteresis may play a role in turbulent-drag reduction, an effect discovered by B. A. Toms a half century ago (*32*): high molecular weight polymers mixed with fluids at an extremely dilute level (~1 part per million by weight) can reduce the drag resistance in turbulent flow by as much as 80% (*33*). Two types of explanations of this effect have been proposed. The first conjecture, originally proposed by Lumley (*34*), argues that the drag reduction occurs at the boundary between the turbulent-core region and the laminar zone near the pipe surface. Polymers that have been extended by (transient) elongational flows can enter the boundary layer and reduce the momentum transfer between the rapidly moving fluid and the laminar layer. Polymers would remain extended for longer periods of time in their stretched state because of conformational-dependent drag. Hysteresis would further magnify this effect. For synthetic polymers that exhibit a large amount of turbulent-drag reduction, $\zeta^{stretch}/\zeta^{coil}$ is estimated to be ~18. In contrast, Tabor and de Gennes have argued (*35*) that polymers in turbulent flows experience rapidly varying extensional flows so that the coil-stretch transition disappears entirely. Instead, they propose that energy is transferred in turbulent flows though a cascade of eddies to smaller size scales where it is finally dissipated. Long polymers interrupt this cascade by storing some of this energy in the form of an elastic modulus that is then delivered back to the moving fluid.

References and Notes

1. R. G. Larson, *The Structure and Rheology of Complex Fluids* (Oxford Univ. Press, New York, 1999).
2. H. P. Babcock, R. E. Teixeira, J. S. Hur, E. S. G. Shaqfeh, S. Chu, *Macromolecules* **36**, 4544 (2003).
3. R. B. Bird, C. F. Curtiss, R. C. Armstrong, O. Hassager, *Dynamics of Polymeric Liquids* (Wiley, New York, ed. 2, 1987), vol. 2.
4. P. G. de Gennes, *J. Chem. Phys.* **60**, 5030 (1974).
5. G. G. Fuller, L. G. Leal, *Rheol. Acta* **19**, 580 (1980).
6. D. Hunkeler, T. Q. Nguyen, H. H. Kausch, *Polymer* **37**, 4257 (1996).
7. M. J. Menasveta, D. A. Hoagland, *Macromolecules* **24**, 3427 (1991).
8. E. C. Lee, S. J. Muller, *Macromolecules* **32**, 3295 (1999).
9. T. T. Perkins, D. E. Smith, S. Chu, *Science* **276**, 2016 (1997).
10. D. E. Smith, S. Chu, *Science* **281**, 1335 (1998).
11. E. J. Hinch, in *Proc. Symp. Polym. Lubrification* **233**, 241 (1974).
12. R. I. Tanner, *Trans. Soc. Rheol.* **19**, 557 (1975).
13. E. J. Hinch, *Phys. Fluids* **20**, s22 (1977).
14. Y. V. Brestkin, *Acta Polymerica* **38**, 470 (1987).
15. J. J. Magda, R. G. Larson, M. E. Mackay, *J. Chem. Phys.* **89**, 2504 (1988).
16. J. M. Rallison, E. J. Hinch, *J. Non-Newtonian Fluid Mech.* **29**, 37 (1988).
17. X. J. Fan, R. B. Bird, M. Renardy, *J. Non-Newtonian Fluid Mech.* **18**, 255 (1985).
18. J. M. Wiest, L. E. Wedgewood, R. B. Bird, *J. Chem. Phys.* **90**, 587 (1988).
19. P. G. de Gennes, *Scaling Concepts in Polymer Physics* (Cornell Univ. Press, Ithaca, NY, 1979).
20. F. Reif, *Fundamentals of Statistical and Thermal Physics* (McGraw-Hill, New York, 1965).
21. G. K. Batchelor, *J. Fluid Mech.* **44**, 419 (1970).
22. We have omitted a numerical constant on the order of unity in this expression.
23. D. E. Smith, T. T. Perkins, S. Chu, *Macromolecules* **29**, 1372 (1996).
24. T. T. Perkins, D. E. Smith, R. G. Larson, S. Chu, *Science* **268**, 83 (1995).
25. DNA molecules were imaged with a Micromax 512BFT camera from Roper Scientific, using a Zeiss Axioplan microscope equipped for epifluorescence with a 40× 1.0 numerical aperture objective oil-immersion lens. We used a 0.31× demagnifying lens to provide a field of view of ≈480 μm. For polymer extensions greater than our field of view, we translated our microscope stage in the direction of molecular stretch to discern total extended lengths. The time scale for translation was on the order of seconds, which was much faster than the time scale of transient molecule dynamics for the range of $\dot{\varepsilon}$ probed.
26. Materials and methods are available as supporting material on *Science* Online.
27. B. J. Bentley, L. G. Leal, *J. Fluid Mech.* **167**, 219 (1986).
28. Polymer relaxation times were measured by first stretching the polymer molecules at high *De* and then stopping the flow. The extent of the visual image of the molecule is tracked as a function of time, and the final 30% of the relaxation is fit to a decaying exponential $\langle x \cdot x \rangle = A\exp(-t/\tau_r) + B$, where x is dimensional polymer extension, τ_r is the longest polymer relaxation time, and A and B are fitting constants. Observation times $t_{obs} = \varepsilon/\dot{\varepsilon}$ on the order of several hours were required for fluid strains of about 10 to 15 units. Therefore, we added a small concentration of Sytox dye (Molecular Probes) to our inlet buffer solutions. Dye molecules bound to DNA exchange with free dye in solution so that fresh dye molecules replenish older, photobleached dye molecules. We also used a mechanical shutter to minimize light exposure from a mercury lamp illuminator and an oxygen-scavenging glucose oxidase–catalase enzyme system to minimize photobleaching. Combining these techniques, we achieved stable polymer relaxation times for at least 7 hours of observation time of a single DNA molecule.
29. R. M. Jendrejack, J. J. de Pablo, M. D. Graham, *J. Chem. Phys.* **116**, 7752 (2002).
30. C. C. Hsieh, L. Li, R. G. Larson, *J. Rheol.*, in press.
31. J. Rotne, S. Prager, *J. Chem. Phys.* **50**, 4831 (1969).
32. B. A. Toms, in *Proc. Int. Congr. Rheol.* **2**, 135 (1949).
33. P. S. Virk, *Am. Inst. Chem. Eng. J.* **21**, 625 (1975).
34. J. Lumley, *J. Polym. Sci. Macromol. Rev.* **7**, 263 (1973).
35. P. G. de Gennes, *Introduction to Polymer Dynamics* (Cambridge Univ. Press, Cambridge, 1990).

36. We thank M. Gallo and E. Chan at U.S. Genomics for generosity in genomic-length *E. coli* DNA sample preparation and G. Fuller and R. Larson for useful discussions. Supported in part by the Materials Research Science and Engineering Center Program of the NSF (DMR-0213618 and DMR-9808677), the Air Force Office of Scientific Research, and the NSF. C.M.S. was supported in part by an NSF graduate fellowship.

Supporting Online Material

www.sciencemag.org/cgi/content/full/301/5639/1515/DC1
Materials and Methods
SOM Text
Figs. S1 to S3

24 April 2003; accepted 8 August 2003

Electronic Structure Control of Single-Walled Carbon Nanotube Functionalization

Michael S. Strano,[1]*† Christopher A. Dyke,[2]* Monica L. Usrey,[1] Paul W. Barone,[1] Mathew J. Allen,[2] Hongwei Shan,[2] Carter Kittrell,[2] Robert H. Hauge,[2] James M. Tour,[2,3]† Richard E. Smalley[2,4]†

Diazonium reagents functionalize single-walled carbon nanotubes suspended in aqueous solution with high selectivity and enable manipulation according to electronic structure. For example, metallic species are shown to react to the near exclusion of semiconducting nanotubes under controlled conditions. Selectivity is dictated by the availability of electrons near the Fermi level to stabilize a charge-transfer transition state preceding bond formation. The chemistry can be reversed by using a thermal treatment that restores the pristine electronic structure of the nanotube.

The main hurdle to the widespread application of single-walled carbon nanotubes is their manipulation according to electronic structure (*1*). All known preparative methods (*2–4*) lead to polydisperse materials of semiconducting, semimetallic and metallic electronic types. Recent advances in the solution-phase dispersion (*5*, *6*), along with spectroscopic identification using band-gap fluorescence (*7*) and Raman spectroscopy (*8*), have greatly improved the ability to monitor electrically distinct nanotubes as suspended mixtures and have led to definitive assignments of the optical features of semiconducting (*7*), as well as metallic and semimetallic, species (*8*).

We now report selective reaction pathways of carbon nanotubes in which covalent chemical functionalization (*9*) is controlled by differ-